PHYSICAL REVIEW E **92**, 011003(R) (2015)

Concentration-dependent diffusion instability in reactive miscible fluids

Dmitry Bratsun,[1] Konstantin Kostarev,[2] Aleksey Mizev,[2] and Elena Mosheva[2]
[1]*Theoretical Physics Department, Perm State Humanitarian Pedagogical University, 614990 Perm, Russia*
[2]*Institute of Continuous Media Mechanics, Academica Koroleva Street 1, 614013 Perm, Russia*
(Received 14 May 2014; revised manuscript received 1 April 2015; published 27 July 2015)

We report on chemoconvective pattern formation phenomena observed in a two-layer system of miscible fluids filling a vertical Hele-Shaw cell. We show both experimentally and theoretically that the concentration-dependent diffusion coupled with frontal acid-base neutralization can give rise to the formation of a local unstable zone low in density, resulting in a perfectly regular cell-type convective pattern. The described effect gives an example of yet another powerful mechanism which allows the reaction-diffusion processes to govern the flow of reacting fluids under gravity conditions.

DOI: 10.1103/PhysRevE.92.011003 PACS number(s): 47.20.Bp, 82.40.Ck, 47.70.Fw, 82.33.Ln

In the past decades the interaction between reaction-diffusion phenomena and pure hydrodynamic instabilities has attracted increasing interests both from a fundamental point of view of nonlinear science and from chemical engineering [1–3]. The interest arises from the fact that the chemically induced changes of fluid properties such as density, viscosity, thermal conductivity, or surface tension may result in instabilities that exhibit a large variety of convective patterns.

The scenario for instability development essentially differs for immiscible and miscible systems of liquids. The simple, irreversible chemical scheme such as a neutralization reaction $A + B \rightarrow S$ occurring in binary liquid-liquid immiscible systems was studied in Refs. [4–10]. The pattern formation in the form of irregular plumes and fingers was shown to originate from the coupling between different gravity-dependent hydrodynamic instabilities occurring when an organic solvent containing an acid A is in contact with an aqueous solution of an inorganic base B [4]. This irregularity looked natural since the configuration of more dense acid on top of a less dense base in the presence of gravity is unstable via the Rayleigh-Taylor (RT) mechanism [5,6]. A much more impressive, regular pattern of cellularlike fingers keeping contact with the interface was reported for an organic base [7]. The regularity was shown to originate from the perfect balance between the RT instability on the one hand, and the Rayleigh-Bénard [8,9] and Marangoni [10] mechanisms on the other. Thus, a liquid-liquid interface has been recognized to be important for performing a fine-tuning of salt fingers.

A completely different situation was observed in the miscible case. The main engine breaking the equilibrium here was found to be the difference between the diffusion rates of all three substances resulting in a double-diffusive (DD) instability or diffusive-layer convection (DLC) as well as RT instability [11]. All the works devoted to this subject, at a given moment, usually noted the formation of irregular patterns of fingers. For example, recently, Almarcha *et al.* [12–14] have shown that various possible convective regimes can be triggered by acid-base reactions when a less dense acid solution lies on top of a denser alkaline one in the gravity field. The possible dynamics is a composition of only two asymptotic cases: irregular plumes induced by a local RT instability above the reaction zone and irregular fingering in the lower solution induced by differential diffusive effects.

In all works in this field, cited or not, the diffusion coefficients of species have been assumed to be constant. Generally, a concentration dependence exists in most systems, but often, e.g., in dilute solutions, the dependence is weak and the diffusion coefficient can be assumed constant [15]. This is especially true for fluid mechanics [16]. Some rare examples of the influence of concentration-dependent diffusion include colloid ultrafiltration [17] and membrane transport [18] where the basic fluid flow is just slightly modified. Reaction-diffusion problems include plasma wave dynamics [19] and the Turing instability under centrifugal forces [20].

In this Rapid Communication, we also focus on the study of chemohydrodynamic processes which accompany a frontal neutralization reaction taking place between two miscible liquids. We report a different type of instability, *concentration-dependent diffusion* (hereinafter CDD) instability from the family of double-diffusion phenomena [21]. It arises when the diffusion coefficients of species depend on their concentrations. We demonstrate both experimentally and theoretically that chemically induced changes of reagent concentrations coupled with concentration-dependent diffusion can produce a spatially localized zone with unstable density stratification that under gravity gives rise to the development of a perfectly periodic convective structure, even in a miscible system.

Experimental results. The experiments were performed in a vertically oriented Hele-Shaw cell made of two glass plates (width 2.5 cm × height 9.0 cm) separated by a thin gap of 0.12 cm. The cell was filled with aqueous solutions of reagents whose concentration always provided a steady stratified density distribution. We examined a few acid-base pairs formed by HCl or HNO_3 from one side and NaOH or KOH from another. During the filling of the cell with the upper solution, the lower layer was separated. The separating mechanism is as follows: Two narrow (approximately 0.3 mm) and not deep (approximately 0.3 mm) slots were made in the glass walls, one opposite another. A thin plastic slide was tightly inserted into the slots, which allowed reliably to separate the reagents before the experiment. In order to start the reaction we took the slide out from the cell.

Fizeau interferometry was used to visualize a refractive index distribution. The latter was caused by inhomogeneities induced by the concentration distribution of species and reaction exothermicity. The maximum temperature increase

measured in the vicinity of the reaction front was found to be near 1 K. In this case the refractive index deviation due to temperature was at least one order of magnitude smaller than that caused by concentration. Thus, the interferograms obtained in the experiments reflected mainly the concentration distribution. Silver-coated hollow glass spheres were added to the liquids to observe the convective patterns which formed during the reaction. We visualized also the pH distribution by adding a small amount of universal acid-base indicator to the solutions. A comparison of the results obtained with and without the indicator shows that the presence of the indicator did not influence the instability scenario and pattern formation process, as it was demonstrated in some recent studies [22,23].

Right after the prepared solutions were brought into contact, the transition zone started to form between them where the reagents were transported towards the reaction front only via the diffusion mechanism. Then, the occurrence of a depleted layer just above the diffusion zone gave rise to the formation of plumes which resulted in the development of weak buoyancy-driven convection in the whole upper layer. A few minutes after the beginning of the experiment, the fluid flow in the form of a periodic array of convective cells [Fig. 1(a)] was formed within the diffusion zone just above the reaction front. The cells were arranged between two areas of immobile fluid, which definitely indicated the formation of a local "pocket" with unstable density stratification [Fig. 1(b)]. One can note that the cellular structure did not interact with the convection in the upper layer. The observations of pH distribution [Fig. 1(c)] show that above and below the cells' band the medium has almost homogeneous pH (acidic or alkaline). The pH within the cellular pattern was more neutral, indicating the accumulation of the reaction product in this zone. The pH images demonstrate the fine structure of the cells' interior. The downstreams of the cells are red (dark in grayscale), indicating that the acid is entrained by the flow. The upstreams are enriched with salt (bright in grayscale), which points out that the reaction occurs at the lower edge of the cellular structure. This is also evidenced by the distribution of the temperature measured along the vertical direction, which indicates the maximum heat output at the lower boundary of the cells. The clearly defined zone of intermediate acidity suggests that we are dealing here with some kind of a cooperative phenomenon. We have found that the cellular structure does not appear if the initial concentration of acid and base is below some threshold, which is approximately equal to 0.75 mol/l.

We have found also that the structure can exist for several hours with the band slowly widening with time [Fig. 1(d)], which results in the wavelength growth [Fig. 1(e)]. It is important to note that this chemoconvective regime was found also in all pairs of reactants used in the experiments, but only at certain ratios of the initial concentrations (Table I).

Theoretical model. To describe the observed phenomenon of CDD instability, we consider two miscible fluids filling a close parallelepiped sufficiently squeezed along one horizontal direction to use a Hele-Shaw approximation [6]. The upper and lower layer are aqueous solutions of acid A and base B, respectively. Right after the process starts, the acid and base diffuse into each other and are neutralized with the formation of salt S with the rate K. The system geometry is given by a two-dimensional domain with the x axis directed horizontally and the z axis antidirected to gravity. We choose the following characteristic scales: The length is the gap width h, time h^2/D_{a0}, velocity D_{a0}/h, pressure $\rho_0 \nu D_{a0}/h^2$, and concentration A_0. Here D_{a0}, ρ_0, ν, and A_0 define the constant acid diffusivity, solvent density, kinematic viscosity, and initial acid concentration, respectively. The mathematical model we

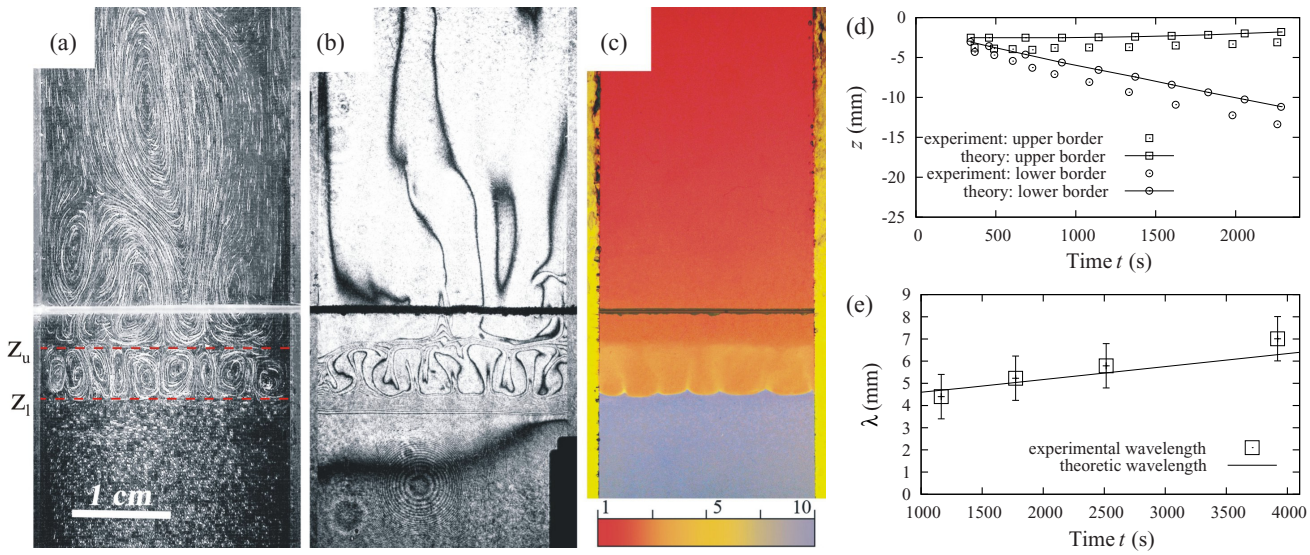

FIG. 1. (Color online) (a)–(c) Chemoconvective structures arising due to the CDD instability observed 1100 s after as the aqueous solutions of HNO_3 (top) and NaOH (bottom) were brought into contact in a vertical Hele-Shaw cell: (a) Velocity field revealed by the tracks of light-scattering particles; (b) interferogram showing a refractive index distribution; (c) pH distribution obtained in the presence of a color indicator. The initial concentrations of the species are both equal to 1 mol/l. The initial contact line is indicated by the horizontal band. (d), (e) Evolution of the upper [indicated in (a) as Z_u] and lower (Z_l) boundaries (d) and wavelength (e) of the CDD pattern in time obtained experimentally (points) and numerically within the theoretical model (lines).

TABLE I. Initial concentration ratios μ of different acid-base pairs for which the cellular chemostructure has been observed.

Acid:Base	HNO_3:NaOH	HNO_3:KOH	HCl:NaOH
μ	1:1	1:1.3	1:0.7

develop consists in a set of reaction-diffusion-convection equations coupled to the Navier-Stokes equation, written in the dimensionless form:

$$\Phi = -\nabla^2\Psi, \tag{1}$$

$$\frac{1}{\mathrm{Sc}}\left(\partial_t\Phi + \frac{6}{5}J(\Psi,\Phi)\right) = \nabla^2\Phi - 12\Phi - R_a\partial_x A - R_b\partial_x B - R_s\partial_x S, \tag{2}$$

$$\partial_t A + J(\Psi,A) = \nabla D_a(A)\nabla A - \alpha AB, \tag{3}$$

$$\partial_t B + J(\Psi,B) = \nabla D_b(B)\nabla B - \alpha AB, \tag{4}$$

$$\partial_t S + J(\Psi,S) = \nabla D_s(S)\nabla S + \alpha AB, \tag{5}$$

where J stands for the Jacobian determinant $J(F,P) \equiv \partial_z F\partial_x P - \partial_x F\partial_z P$. Here, we use a two-field formulation for the motion equation, and introduce the stream function Ψ and vorticity Φ defined by (1). Equation (2) differs from a standard Navier-Stokes equation by the additional term 12Φ, which is responsible for the average friction force due to the presence of the sidewalls. Diffusion terms in Eqs. (3)–(5) have been written in the most general form [15].

The problem parameters are the Schmidt number $\mathrm{Sc} = \nu/D_{a0}$, the Damköhler number $\alpha = KA_0h^2/D_{a0}$, and the set of solutal Rayleigh numbers for species $R_i = g\beta_i A_0 h^3/\nu D_{a0}$, $i = \{a,b,s\}$. Their values for the pair HNO_3/NaOH (see Table I) have been estimated as follows: $\mathrm{Sc} = 10^3$, $\alpha = 10^3$, $R_a = 1.5\times10^3$, $R_b = 1.8\times10^3$, $R_s = 2.4\times10^3$.

The boundary conditions for Eqs. (1)–(5) are

$$\Psi = 0, \quad \partial_i\Psi = 0, \quad \partial_i A = 0, \quad \partial_i B = 0, \quad \partial_i S = 0, \tag{6}$$

where $i = \{x,z\}$ for sidewalls and horizontal boundaries, respectively. The initial conditions at $t = 0$ are as follows:

$$\begin{aligned} z \leqslant 0: &\quad \Psi = 0, \quad \partial_z\Psi = 0, \quad A = 0, \quad B = 1; \\ z > 0: &\quad \Psi = 0, \quad \partial_z\Psi = 0, \quad A = 1, \quad B = 0. \end{aligned} \tag{7}$$

We have found that a concentration dependence of diffusion plays an important role in the pattern formation. Thus, in Eqs. (3)–(5) the diffusion coefficients have been assumed to be not constant, but to depend on their own concentration: $D_a(A)$, $D_b(B)$, and $D_s(S)$. In order to evaluate the diffusion formulas for the pair HNO_3/NaOH, we have brought together all of the experimental data known to us. It should be noted that the data on the concentration dependence of the diffusion coefficients have appeared to be fragmentary and incomplete for most substances. Even the simple and commonly used chemical substances such as nitric acid and its salt are poorly investigated. This proves indirectly that the CDD effect has yet to be claimed in the fluid mechanics.

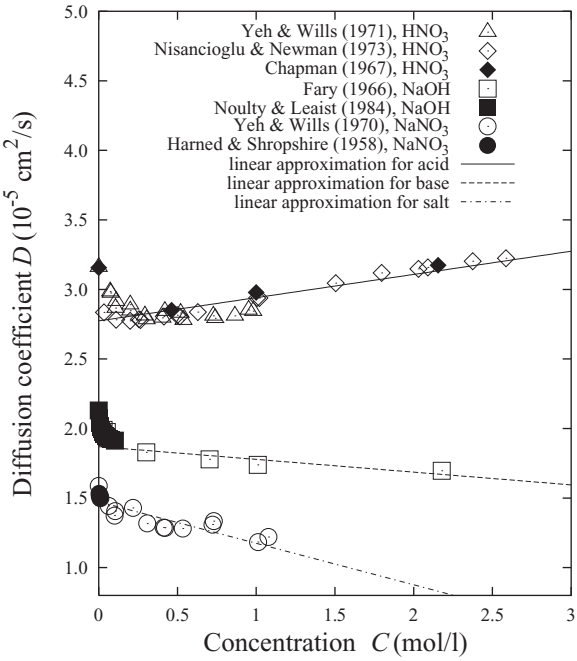

FIG. 2. Observed diffusion coefficients for nitric acid, sodium hydroxide, and their salt in aqueous solution at 25 °C as a function of the concentrations of diffusing substances $C = \{A,B,S\}$ are indicated by points. The straight lines represent the least-squares fit to the experimental data set.

Figure 2 represents the values of the diffusion coefficients for nitric acid HNO_3, sodium hydroxide NaOH, and their salt $NaNO_3$ in an aqueous solution at 25 °C reported in Refs. [24–30], respectively. We have assumed for simplicity that in the experimentally interesting range of concentration (from 0.1 to 3 mol/l, as seen in Fig. 1) the observed data set falls on a straight line, $f(x) = \alpha x + \beta$, where α and β are constants. By applying the linear least-squares method, one can obtain

$$\begin{aligned} D_a(A) &\approx 0.158A + 0.881, \\ D_b(B) &\approx -0.087B + 0.594, \\ D_s(S) &\approx -0.284S + 0.478. \end{aligned} \tag{8}$$

In contrast to (8), the constant table values of diffusion coefficients taken from Ref. [31] are

$$D_a^{\mathrm{tab}} = 1, \quad D_b^{\mathrm{tab}} = 0.68, \quad D_s^{\mathrm{tab}} = 0.5. \tag{9}$$

Formulas (8) do not reproduce values (9) in the case of zero concentrations, because for small concentration values the diffusion coefficients decrease dramatically, making a linear approximation insufficient. However, this effect only occurs at very small concentrations of reactants that can be neglected for most cases (Fig. 2).

It follows from (8) that the salt is most immobile, compared with the acid and base. In addition, the diffusivity of salt decreases with the growth of the salt concentration. All these factors together produce an interesting effect. In order to describe it in terms of the buoyancy, it is convenient to introduce the total dimensionless density,

$$\rho(x,z) = R_a A(x,z) + R_b B(x,z) + R_s S(x,z). \tag{10}$$

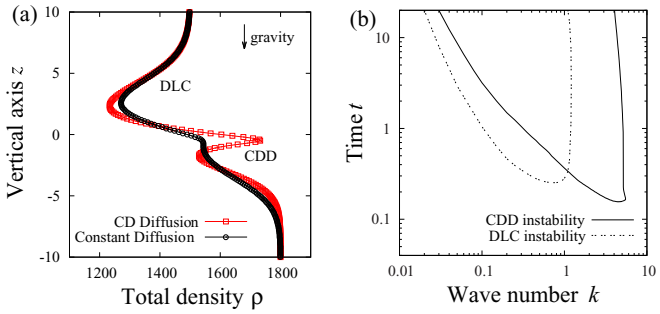

FIG. 3. (Color online) (a) Instantaneous base state profiles of the total density (10) for the case of constant diffusion (black circles) and concentration-dependent diffusion (red squares) at $t = 5$; (b) neutral curves for DLC and CDD instabilities which arise in two zones low in density, shown in (a).

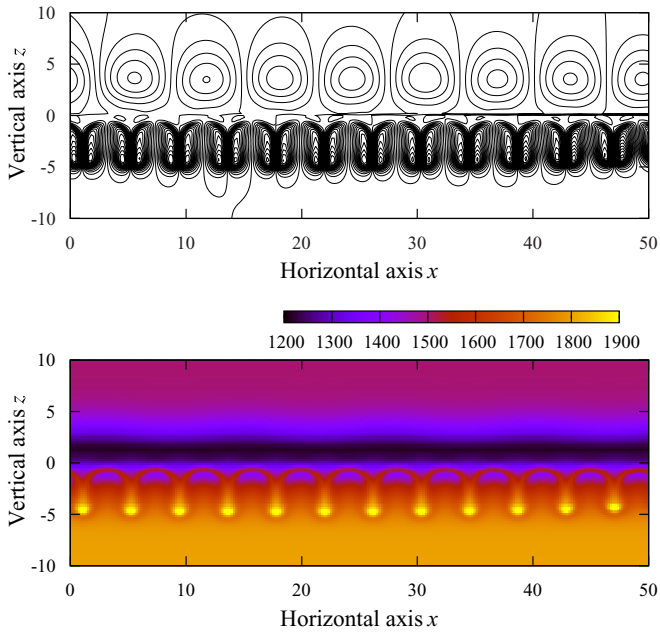

FIG. 4. (Color online) Stream function (top) and total density (bottom) obtained by numerically solving a full nonlinear set of equations (1)–(8) for time $t = 3$. The line $z = 0$ corresponds to the initial contact line between layers. Nonlinear development of the CDD instability below the contact line is clearly seen.

The base state profiles for the density (10) are shown in Fig. 3(a) for two different diffusion laws: (i) the constant diffusion with standard table values for coefficients defined by (9), and (ii) the concentration-dependent diffusion defined by (8). We see that the curve has only one minimum above the reaction front in case (i) versus two minima (above and below the reaction front) in case (ii). The lower minimum enclosed within the regions with a stable stratification occurs because of the progressively slower diffusion of the salt, resulting in its accumulation in or near the reaction front. Both minima enable for the potential development of the instability in the presence of gravity. The upper minimum is the typical for the DLC instability [Fig. 3(a), squares]. The lower local minimum on the same curve is much more interesting: Since it has appeared exclusively due to the concentration dependence of diffusion, we have named it the CDD instability.

A nonsteady spectral amplitude problem has been solved by the method suggested originally in Ref. [32] and developed for chemoconvection in Refs. [8,10]. Figure 3(b) shows the neutral curves for the DLC and CDD instabilities. At time $t \approx 0.15$ the CDD disturbance with a wave number $k \approx 4.6$ is the first to lose stability. Then more and more waves are involved in the instability area. The DLC instability arises at $t \approx 0.25$, and its critical wave number at the very beginning is $k \approx 0.75$. Eventually the maximum growth rate of disturbances in the instability balloon is shifted towards longer wavelengths.

To see the nonlinear development of the disturbances, the problem (1)–(8) has been solved numerically by a finite-difference method described in detail in Ref. [8]. Stream lines and the total density of the pattern at time $t = 3$ are presented in Fig. 4. We found that in both zones low in density the convection develops independently (Fig. 4, top). The most interesting situation is in the lower area, where the cellular chemoconvection with a perfectly periodic structure induced by the CDD instability has been observed. As in the experiment, the boundaries of the structure slowly move apart with time [Fig. 1(e)]. At $t = 3$ the pattern wavelength is about 4.2, which is in good agreement with the experimental data [Fig. 1(d)].

Discussion and closing remarks. The system of miscible fluids when a given solution is placed above a denser solution with the fastest diffusing species in the upper layer has been classified in Ref. [11] as a typical case of DLC instability. It occurs due to the formation of a depleted zone low in density which develops above the initial contact line while an accumulation zone where the density is maximal is obtained below the line. As a result, irregular DLC fingering is observed which develops on both sides of the initial contact line. In our case we also can identify the DLC plumes above the initial reaction front [see the upper zone in Figs. 1(a) and 4]. But below the contact line we see a different kind of instability. It may occur only in the reactive case when an emerging component starts to accumulate near the reaction front. If its molecules quickly leave the reaction zone, then it has no significant influence on the instability scenario. But if the diffusion coefficient of the reaction product decreases with growth of its concentration (the CDD effect), it can progressively make a local minimum in the density profile (figuratively, a "density pocket"). Finally, under gravity conditions, one can observe the development of localized cellular convection within the bulk of the motionless liquid [see the lower zone in Figs. 1(a) and 4].

After the localized CDD structure was occasionally found in the pair HNO_3/NaOH, we have tested a number of other systems and found a similar patterning there. In our opinion, it may indicate that the discovered effect is of a general nature and should be taken into account in reaction-diffusion-convection problems as another tool to organize the movement of the reacting fluids. We have noted above that the data on the concentration dependence of the diffusion coefficients are incomplete even for the most simple substances. We hope that our work will stimulate research in this direction. Finally, the CDD effect should take its place among other instabilities (DD,

DDD, and DLC) of the family of double-diffusive phenomena introduced in physics over 60 years ago [21].

Acknowledgments. We wish to thank A. De Wit, K. Eckert, and L. Pismen for stimulating discussions. The work was supported by the Perm Regional Ministry of Education and Science (MIG's Project No. C-26/004.4), Russian Fund for Basic Research (13-01-00508a, 14-01-96021r_ural_a), and Basic Research Program of UB RAS (No. 15-10-1-16).

[1] D. Avnir and M. L. Kagan, Chaos **5**, 589 (1995).
[2] A. J. Pons, F. Sagues, M. A. Bees, and P. G. Sorensen, J. Phys. Chem. B **104**, 2251 (2000).
[3] Y. Shi and K. Eckert, Chem. Eng. Sci. **63**, 3560 (2008).
[4] K. Eckert and A. Grahn, Phys. Rev. Lett. **82**, 4436 (1999).
[5] D. A. Bratsun and A. De Wit, Tech. Phys. **53**, 146 (2008).
[6] D. A. Bratsun and A. De Wit, Chem. Eng. Sci. **66**, 5723 (2011).
[7] K. Eckert, M. Acker, and Y. Shi, Phys. Fluids **16**, 385 (2004).
[8] D. A. Bratsun, Microgravity Sci. Technol. **26**, 293 (2014).
[9] D. A. Bratsun, J. Appl. Mech. Tech. Phys. **55**, 199 (2014).
[10] D. A. Bratsun and A. De Wit, Phys. Fluids **16**, 1082 (2004).
[11] P. M. J. Trevelyan, C. Almarcha, and A. De Wit, Phys. Rev. E **91**, 023001 (2015).
[12] C. Almarcha, P. M. J. Trevelyan, P. Grosfils, and A. De Wit, Phys. Rev. Lett. **104**, 044501 (2010).
[13] C. Almarcha, Y. R'Honi, Y. De Decker, P. M. J. Trevelyan, K. Eckert, and A. De Wit, J. Phys. Chem. B **115**, 9739 (2011).
[14] J. Carballido-Landeira, P. M. J. Trevelyan, C. Almarcha, and A. De Wit, Phys. Fluids **25**, 024107 (2013).
[15] J. Crank, *The Mathematics of Diffusion* (Clarendon, Oxford, UK, 1975).
[16] G. K. Batchelor, *An Introduction to Fluid Dynamics* (Cambridge University Press, UK, 2000).
[17] W. R. Bowen and P. M. Williams, Chem. Eng. Sci. **56**, 3083 (2001).
[18] R. Ash and S. E. Espenhahn, J. Membr. Sci. **180**, 133 (2000).
[19] P. Rosenau, Phys. Rev. Lett. **88**, 194501 (2002).
[20] J. Guiu-Souto and A. P. Muñuzuri, Phys. Rev. E **91**, 012917 (2015).
[21] J. S. Turner, Annu. Rev. Fluid Mech. **6**, 37 (1974).
[22] C. Almarcha, P. M. J. Trevelyan, L. A. Riolfo, A. Zalts, C. El Hasi, A. D'Onofrio, and A. De Wit, J. Phys. Chem. Lett. **1**, 752 (2010).
[23] S. Kuster, Phys. Chem. Chem. Phys. **13**, 17295 (2011).
[24] T. W. Chapman, Ph.D. thesis, University of California, Berkeley, 1967.
[25] H.-S. Yeh and G. B. Wills, J. Chem. Eng. Data **16**, 76 (1971).
[26] K. Nisancioglu and J. Newman, AIChE J. **19**, 797 (1973).
[27] A. D. Fary, Ph.D. thesis, Institute of Paper Chemistry affiliated with Lawrence College, Appleton, WI, 1966.
[28] R. A. Noulty and D. G. Leaist, J. Solution Chem. **13**, 767 (1984).
[29] H. S. Harned and J. A. Shropshire, J. Am. Chem. Soc. **80**, 2618 (1958).
[30] H.-S. Yeh and G. B. Wills, J. Chem. Eng. Data **15**, 187 (1970).
[31] *CRC Handbook of Chemistry and Physics*, edited by D. R. Lide (CRC Press, Boca Raton, FL, 2011).
[32] C. T. Tan and G. M. Homsy, Phys. Fluids **29**, 3549 (1986).